Proceeding of the IEEE
International Conference on Robotics and Biomimetics
Dali, China, December 2019

A Proposal of the Kinematic Model of the Horse Leg Musculoskeletal System by Using Closed Linkages*

Dondogjamts Batbaatar†
†Graduate School of Life Science and Systems Engineering
Kyushu Institute of Technology
Wakamatsu-Ku, Kitakyushu, Japan
batbaatar.dondogjamts581@mail.kyutech.jp

Hiroaki Wagatsuma†‡§
† Graduate School of Life Science and Systems Engineering
Kyushu Institute of Technology, Japan
‡RIKEN Center for Brain Science, Saitama, Japan
§Artificial Intelligence Research Center, AIST, Tokyo, Japan
waga@brain.kyutech.ac.jp

Abstract*- In part, closed loop mechanisms can be found in musculoskeletal systems in animals, which are not only composed of combinations with bones and muscles but also of tendons in proper positions. Indeed, the mechanism provides flexible animal gait patterns which is associated with different leg trajectories depending on the ground condition and the purpose. In this paper, we focused on the horse leg mechanism as an animal to be able to adapt to the guidance of the house rider and hypothesized that the principle mechanism can be modeled with closed linkages with a changeable length link, which is formulated as a distance driver. The horse hind limb is driven in a complex manner by kinematic joints and forces generated by muscles and tendons, while in the viewpoint of the geometrical structure of principal joints were selected from the original structure and coupling with other reconstructed linkages as a simple form. In the computer experiment based on the multibody dynamics, the proposed linkage system demonstrated that horse leg-like trajectories were provided by the proposed model with eleven fixed links and a relative distance driver as a function of muscle-tendon unit. In the closed linkage, a uniform circular motion is assumed in the input driving force and the force is transmitted to the end-effector as toe and then a desired locomotive trajectory is provided. The important finding is that a kicking force is generated in the toe just before the grounding. This non-linear kinematic transmission may provide a hint to analyze adaptive capabilities in the animal locomotion even by the simple closed linkage without a complex actuator control system.

Keywords—Musculoskeletal system, Closed loop linkage, Kinematic transmission, Biological motion, Walking machine.

I. INTRODUCTION

Legged locomotion has been widely studied and tried to rebuild by simple mechanical systems called biological walkers, which were based on open and closed chain mechanical systems [1-4]. Biological walkers are not only focusing on a benefit of multiplicity of legs [2, 4], but also are highlighted in a less- energy consumption according to the generation of smooth leg trajectories, which is demonstrated by Theo Jansen [5] by using the closed linkage system with eleven links and the energy-efficacy was theoretically proved by Komoda and Wagatsuma [6] in comparison with biological walkers measured by specific resistance (SR) by using multibody dynamics [7, 8]. They analyzed that the Theo Jansen mechanism walks with less energy consumption with respect to hexapods [2, 4] when it is moving with a slow walking speed, while it is getting worse in the high-speed walking. However, it is known that the animal locomotion changes depending on the speed of mobility, especially in horses, which exhibit gait pattern transitions [9-12], presumably for minimization of the energy consumption. In the consideration of analyses on the energy efficacy of the animal locomotion with a high-speed mobility, the kinematic model based on a simple mechanism such as closed linkages has advantages [6] yet it requires the mechanism with a high duty-factor [11, 13], which is defined as the fraction of the duration of a stride for which each foot remains on the ground, or the ratio between stance and swing phase. Interestingly, possible extensions of closed linkage mechanism were reported [14-16] in order to change the duty-factor.

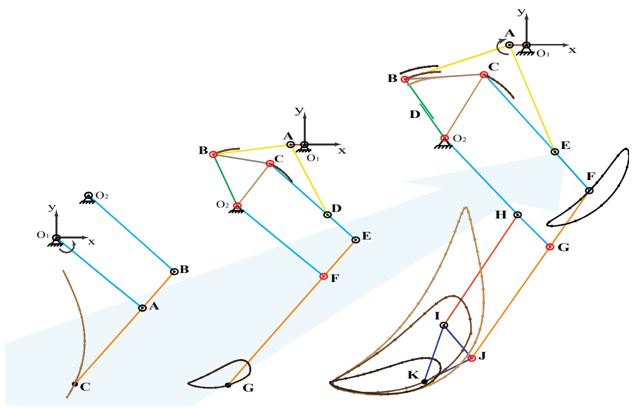

Fig. 1 Implementation of horse leg mechanism. Proposed leg mechanism consists of three parts: Reciprocal mechanism, which observed in horse hind limb produces lifting up motion in lower part of the leg. Theo-Jansen like simplified mechanism with cyclic driving unit. Horse like Leg mechanism with different modifiable footpath, linear actuator inserted and hoof mechanism added based on anatomy of the horse leg.

*This work is partially supported by JSPS Kakenhi (15H05874, 16H01616, 17H06383), LORIA-Kyutech collaboration research project and the New Energy and Industrial Technology Development Organization (NEDO).

978-1-7281-6321-5/19//$31.00 ©2019 IEEE

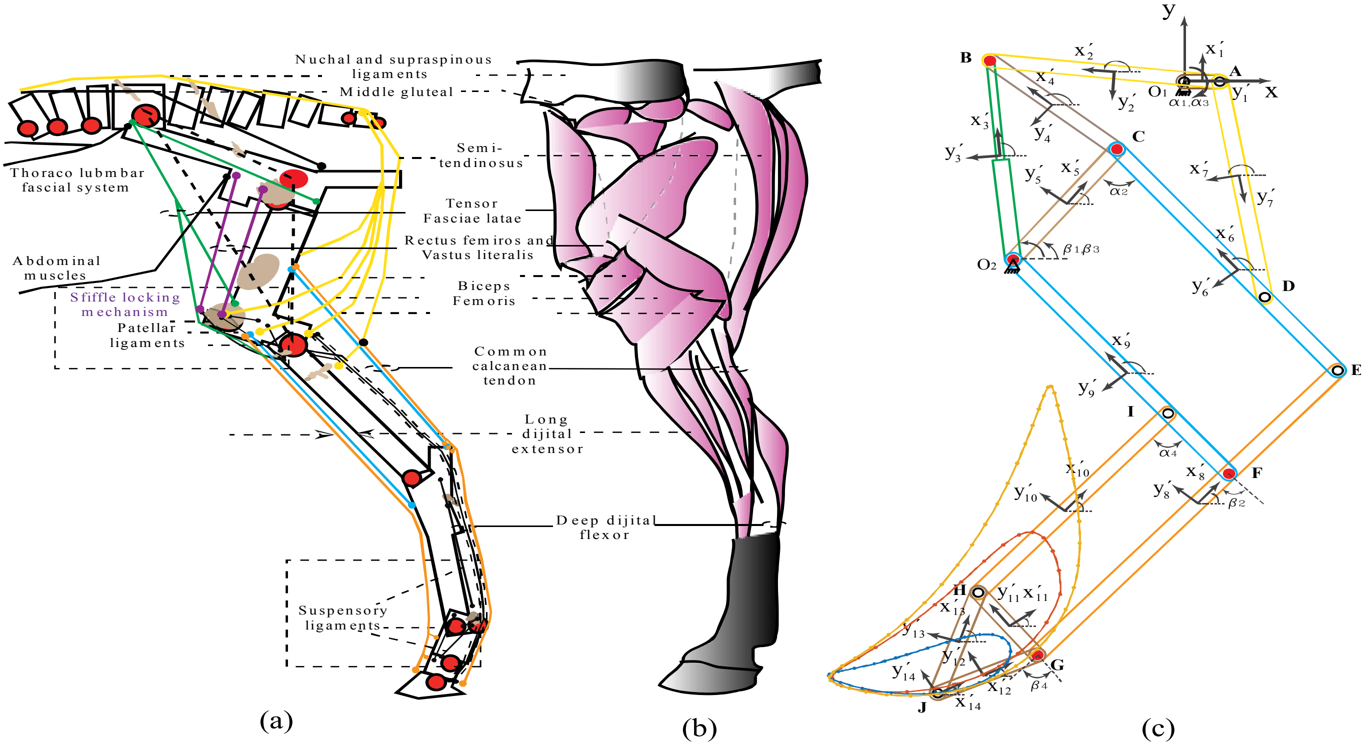

Fig. 2 Schematic illustration of the musculoskeletal system of the horse hind limb (a) Associations of bones and joint positions, (b) the muscle organization and (a) the proposed model with closed linkages. Figures (a) an (b) were drawn based on analyses of Budras et al. (2012) [18].

Interestingly, Coros et. al. [17] propsed the theoretical framework to provide a desired cyclic trajectory based on multiple gears with different diameters and rotation phases connected with linkages by using a solver of the constraint optimization problem and then verified to provide animal leg motions. Their approach has an advantage of the design any free form of cyclic motion can be generated by the combination of multi-gears with a simple linkage as the kinematic analysis; however their theoretical analysis cannot apply to computation of the force and torque estimation of the mechanism as the kinetical analysis. In the sake of kinematic and kinetical analysis of the horse leg motion as the representative animal with a high-speed mobility, we hypothesized that the musculoskeletal system can be modeled based on closed linkages as shown in Fig.1 and found a critical link to effectively control the shape of leg trajectories. Once the functional relationship of muscle-tendon units can be represented by the simple closed-linkage system, the model allow us to investigate how the leg trajectory is modifiable in the displacement analysis in the kinematic analysis and when and where the leg has the maximum torque in the inverse kinematic analysis. This method will reveal what kinematic transmission are derived from the input to the end-effector as toe by applying changes of parameters to represent leg components.

This paper was organized as follows. Section II explain anatomical structure of horse hind limb and a possible interpretation as linkages. Section III introduces theoretical and computational method as multibody dynamics to validate the effectiveness of leg mechanism. The next section explains linkage-type analysis focusing on the kinematic transmission. In addition, system characteristic analysis of the proposed leg mechanism including the torque evaluation along the leg trajectory. Finally, Section V discusses the conclusions and future work.

II. Anatomy of the Horse Leg

In the horse body, reciprocal mechanism in hind limb, basics of functional anatomy observed in vitro experiment [19], confirmed by vivo measurement [20] are shown in Fig. 2 (a), (c) with blue and orange lines to represent the stifle and the hock move individually. The mechanism produces a lifting-up trajectory that allows the horse to navigate the lower limb in a smooth and coordinated manner as shown in Fig.1 (c). Mechanics of the horse leg was explained by Hoyt et. al. [10] and Hildebrand [21] with its anatomical point of view. A purely qualitative investigation of rear-leg external anatomy shows a similarity in this proposed design in shape and size of the distal region, while that the proximal limb (rump) is larger and more rounded than the equivalent shoulder region indeed. Fig. 2 (a) and (b) provided the musculoskeletal structure of whole hind limb which we focused on. The red circles represent joints in horse limb correspond to the B C, O2, F, G joints in proposed leg mechanism except the joints placed in suspensory part. Musculoskeletal structure of hind limb was represented by simple shapes such as triangle in upper limb dotted by big red circles in Fig. 2(a), which is controlled by tensor fasciae muscles and series parallelogram in lower limb represented by blue and orange colors known as reciprocal apparatus. The triangle structure in the toe which contacts with the ground known as hoof formed by links drawn by orange lines except to the suspensory ligaments. Thus, all of these connections provides the unique structure of walking in the viewpoint of closed linkages. It leads an operating principle of the horse leg mechanism to have an upper and lower 3-bar mechanism forms a rigid triangle that allows parallelogram linkage to change the shape and guide motion of one another. Finally, motion transferred from second parallelogram to the hoof part. Same principle operates in the Theo-Jansen mechanism [14-16] in case of simplified model illustrated in Fig. 1(b). However, none of related past related works [14-16] have not yet reported the importance of an additional linear translational actuator, which is critically control the shape of the leg trajectory. We focused on the original perspective and applied this principle to reciprocal apparatus and the hoof part in proposed leg mechanism in Fig. 2(c). In the following section, the function was evaluated with multibody dynamics.

III. FORMULATION OF THE HORSE LEG MECHANISM WITH MULTIBODY DYNAMICS

In the horse body, reciprocal mechanism in hind limb is highly important. In order to generate a horse walking motion the mechanism requires seventeen number of bodies including ground and guided by absolute rational and relative distance driver. Therefore, general approach [22] leads to a sparse matrix structure in constrained multibody system used to validate the mechanism in this section. Firstly, the DOFs of the linkage mechanism can be evaluated according to the mobility criterion:

$$n_d = 3 \times n_b - n_c \tag{1}$$

where n_d is the number of the system degree of freedom, n_b is the number of bodies in the system, and n_c is the total number of linearly independent constraint equations that describe the joint is in the system. Each revolute and linear translation joint reduces DOF by two. The overall number of DOFs n_d obtained using Eq. (1) is two. Secondly, flowchart of the computational strategy for dynamic analysis of constrained multibody system described as follows:

TABLE 1. PARAMETERS USED IN THE NUMERICAL SIMULATION

Parameters	Description	Value
g	Gravitational acceleration	9.81 m/s^2
ω	Input angular velocity	2 rad/s
t	time	$0 \le t \le 4s$
α	Constraint stabilization Baumgarte parameters	15
β		$\sqrt{2\alpha}$
dt	Time step	$1.0\times10^{-3}\,s$
-	Solution ODE	Euler's method

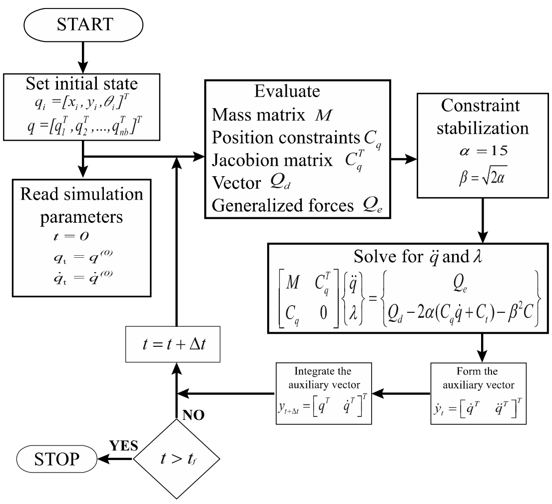

Fig. 3 Flowchart of iterative procedure for dynamics analysis of multibody systems with constraint stabilization Baumgarte method

MATLAB-based numerical simulations were performed, according to the parameters given in Table 1. Initial condition of the mechanism was given by set of the vector of generalized coordinates on the center of all bodies. The following steps were done in the iterative computational procedure of motion equation presented (Fig. 3):

1. Start instant of time t^0 with given initial condition for position q^0 and velocities q^0.

$$q = [q_1^T, q_2^T, \ldots, q_{nb}^T]^T_{14\times1} \tag{2}$$

where $q_i = [R_i^T \quad \phi_i]^T$ is the vector of planar Cartesian generalized coordinates for a multibody dynamics system.

2. Assemble global mass matrix M (42 × 42) position constraint equation C_q (42 × 1)and Jacobian matrix C_q^T. Determine the right-hand side of the acceleration Q_d, and calculate the generalized external forces Q_e (42×1) are described as follows:

$$M = diag(M_1, M_2, M_3, \ldots M_{14}), \tag{3}$$

$$\{M_i = [m_i, m_i, J_i]^T \mid i = 1, \ldots 14\}, \tag{4}$$

$$C_q = \begin{bmatrix} C_K(q) \\ C_{rd}(q,t) \end{bmatrix} = 0, \tag{5}$$

$$C_q^T = \left[\frac{\partial C(q,t)}{\partial q}\right]_{42\times42}, \tag{6}$$

$$C_q\ddot{q} =-(C_q\dot{q})_q\dot{q} - 2C_{qt}\dot{q} - C_{tt} \equiv Q_d, \tag{7}$$

$$Q_e = [Q_1^{e\,T}, Q_2^{e\,T}, \ldots, Q_{14}^{e\,T}]^T, \tag{8}$$

$$\{Q_e^i = [0, -m_i g, 0]^T \mid i = 1, \ldots, 14\}, \tag{9}$$

In Eq. (5) $C_K(q)$ is kinematic constrains and $C_{rd}(q,t)$ denotes the rotational driver constraint, which specifies relative motion between two bodies written as:

$$C_{rd} = \varphi_i - \varphi_j - f(t) = 0 \tag{10}$$

$C_{dd}(q,t)$ is relative distance driver as a lettered D on Fig. 1(c) which is newly introduced in this linkage system together with rotational driver formulated as follows:

$$C_{dd} = d_{ij}^T - f(t)^2 = 0 \tag{11}$$

where $d_{ij}^T = r_j + s_j^p - r_i - s_i^p$ is distance between a point P_i in body i and point P_j in body j is specified in mechanical system connected by revolute joints.

3. Solve the mixed set of differential algebraic equations of motion for acceleration $\ddot{q}$ and Lagrangian multiplier λ at instant t as shown in Fig. 3. Where α and β are positive feedback coefficients which are the damping ratio and natural frequency in the dynamic behavior of this equation firstly introduced by Baumgarte [23]. Effect of stabilization studied on Ostermeyer [24]. It is noted that *α*

and β used on maintaining stability in numerical simulation and well-known Baumgarte parameters are different from motion variables used on upcoming sections.

4. Assemble the vector $\dot{y}_t$ containing the generalized velocities $\dot{q}$ and accelerations $\ddot{q}$ for instant of time t.

5. Integrate numerically, vector $\dot{q}$ and $\ddot{q}$ with time step $t + \Delta t$ and obtain the new position and velocities.

6. Update the time variable until simulation reach to the end.

System has two degree of freedom. However, initial state of mechanism calculated before the simulation for all three trajectories. Simulation made on three different constant value of the length of L_3 link. According to the inverse dynamics analysis following rearranged differential algebraic equation solved for driving torque:

$$\tau = \frac{\dot{q}'(M\ddot{q} - g)}{D\dot{q}} \tag{12}$$

where τ is the driving torque and D is the Jacobian of the driver constraints. Finally, power of the driving crankshaft described as follows:

$$P = \tau\omega \tag{13}$$

IV. RESULT AND DISCUSSION

A. *CLASSIFICATION OF ENGINEERING AND BIOLOGICAL LINKAGE IN HORSE LEG MECHANISM*

Except for the engineering classification of the planar linkages driven by cyclic motion as known as Grashof condition, Muller (1996) [25] proposed the analytical classification method focusing on evolutionary changes in the mechanical behavior of the biological linkages. Its linear and non-linear transmission property indicated in living organisms with different parameter such as length and absolute angle. According to the classification, the reciprocal mechanism in horse hind limb based on its anatomical name of the bars coded in type of '2Plsls' parallelogram linkage. Here number indicates the motion variables and linkage is non-crossed parallelogram based on their length of the bars a≅c and b≅d, where 'a, c' are the length of long side as noted O_2 to F and E to C as shown in Fig. 2 (c). The configuration gives a linear transmission of α_2 to β_2 (α-input angle, β-output angle).

TABLE 2. LINKS IN HORSE HIND LIMB MECHANISM

Parameters		3 bars		Parallelogram -1		5 bar		Parallelogram -2		Foot link
Sides		O_1-A-B-O_2		O_2-F-E-C-D- O_2		O_1-A-D-C-O_2		I-F-J-H-I		J-H-G-J
Distance driver		ΔL_{3min}	ΔL_{3max}	ΔL_{3min}	ΔL_{3max}	ΔL_{3min}	ΔL_{3max}	ΔL_{3min}	ΔL_{3max}	ΔL_{3min}
$\alpha_{1,2,3,4,5}$		0°-360°		51.6°-141°	35.9°-86.7°	0°-360°		51.1°-145°	34.5°-87.6°	107.4°-169.7°
$\beta_{1,2,3,4,5}$		94 °-124°	96 °-114°	50.8°-139°	35.0°-86.0°	29.5°-60.3°	51.5°-69.9°	49.7°-140°	33.1°-85.7°	7.0°-69.33°
Kinematic Transmission	Non-linear	✓				✓				
	Linear			✓				✓		✓
Types of the linkages according to Muller [24]		Crank and rocker-cr		2Plsls		5R		2Plsls		Foot
		Engineering		Biological		Engineering		Biological		Biological

A positive transmission α, β either increases or decreases of the type '2Plsls', absolute transmission stability obtained in biological system. Working range of output motion variable indicated [30°-145°] in case of the biological linkage driven by muscles in horse hind limb [19]. Before making the classification of mechanism into biological and engineering linkages, we tested the effect of length changes of L_3 link. Besides, L_3 is the linear actuator connecting B and O_2 grounded node as shown in Fig. 2(c), x_3' and y_3' are coordinates located in the center of the body correspond to the absolute coordinates defining orientation of the body. Table 2. Shows the experimental result of classification for all linkages entered in proposed leg mechanism. Firstly, linear transmission observed in biological linkage. The range of the motion variables α_2, β_2 of "2Plsls" linkage indicated [35°-141°], which was close to its working range of biological linkage as previously mentioned. Secondly, Non-linear transmission depending on length of linear actuator L_3 was observed in engineering linkages.

Kinematic transmission of the crank-rocker mechanism measured by input angle α_1 output angle β_1 as shown in Fig. 4. As a result, the amplitude of angular oscillation in rocker link changes depending on length of L_3 link. In addition, amplitude measured on three different values of L_3 link, black triangle correspond to the highest points of the oscillation and red dot represent the lowest points. All the links in this leg mechanism controlled by one another. Therefore, the relative angle between them describes the amplification of force and speed and acceleration of end effector.

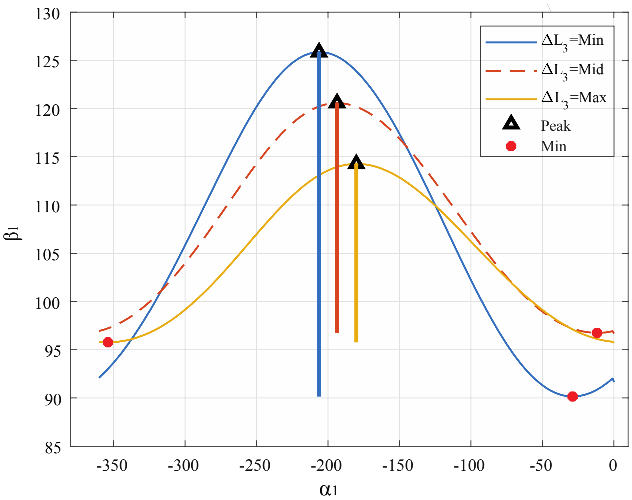

Fig. 4 An effect of length changes of the L_3 link in proposed leg mechanism

B. CHARACTERISTIC ANALYSIS

According to the MBD descriptions as previously mentioned, characteristic analysis can be treated by numerically, which allows for investigation of the temporal evaluation of placement, posture, velocity, and torque in every joint.

In the kinematic analysis, common factors were displayed by different colors respect to the length of L_3 link as shown in Fig. 5. Minimum velocity estimated 1.08 m/s regards to the maximum length, which is consistent for energy efficient walking. According to the end-effectors placement on the Fig. 2 (c) that the mechanism produces three different trajectories respect to length of distance driver, each trajectory had different characteristic. However, duty factors respect to the trajectories were close to each other 0.1782, 0.227, and 0.3267, which are representative of running behavior. The height of the trajectories were computed 0.073, 0.1924 and 0.281 m from center second grounded revolute joint $O_2=(-0.12, -0.15)^T$ to the lowest point of the foot trajectory. All these factors indicated that linearly dependent to the length of distance driver and shown variety of different values represented. Torque analysis defined by Eq. (12). Furthermore, power consumptions were obtained from multiplication of driving torque τ and angular velocity ω, which was set constant in this analysis, as defined in Eq. (13).

Velocity and acceleration of the leg mechanism illustrated on Fig. 6 (b), (c) when the length of distance driver is equal to its medium length, analysis result were plotted by using absolute values of $\sqrt{\dot{x}^2+\dot{y}^2}$ and $\sqrt{\ddot{x}^2+\ddot{y}^2}$ with respect to the time. Velocity result showed that speed increases gradually before grounding and decreases rapidly as soon as leg touches on the ground, which is indicator for separation of stance and swing as shown in Fig.6 (a). More clear separation made on timing as shown in Fig.6 (d) and positive torque was observed at the swing phase whereas negative torque was observed when the leg is on the ground at stance phase. An acceleration analysis showed that mechanism moves fast when leg takes off the ground and maximize the acceleration before grounding as shown in Fig.6 (b).

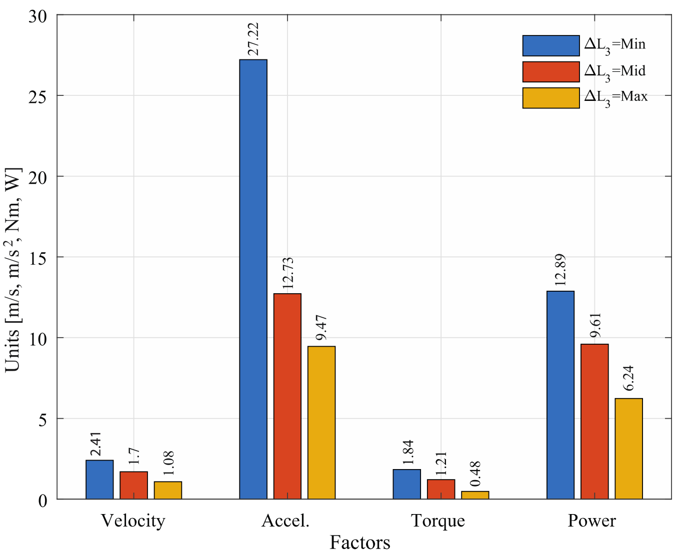

Fig. 5 Comparison of the common factors in relation to length of L_3 link

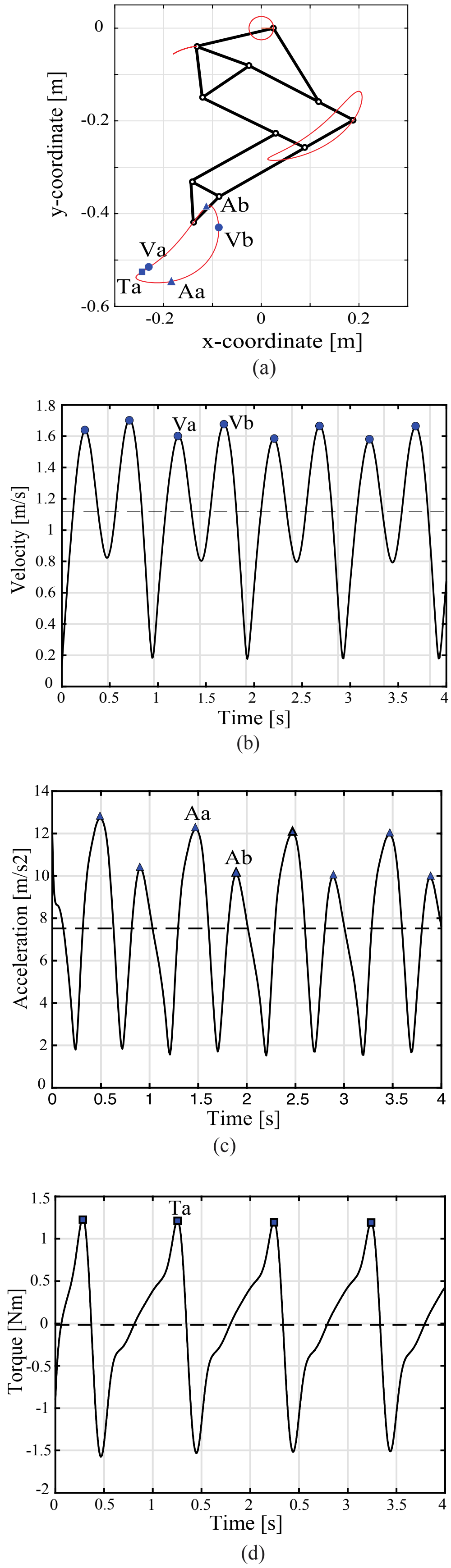

Fig. 6 Characteristic analysis including end effectors placements in the case of Δ_3 =ave (average). (a) the planner trajectory is shown in, (b) velocity analysis, (c) acceleration, (d) and driving torque τ of the proposed leg mechanism.

The inference 'Walking machines should be capable of changing their height of step relative to the ground' was important to consider basic requirements for judging or rating the various walking mechanisms investigated by mechanical walker pioneer, Joseph Shigley [26].

This result suggested that the proposed linkage mechanism can be compared with other proposed linkage mechanism such as Klann and Theo Jansen as compared in Komoda and Wagatsuma [6] and has a common property with multiple mechanisms depending on the length change of L_3 link, which we called the relative distance driver. If the hypothesis is true, the energy consumption can be controlled by the simple manner as the change of the length of the critical link.

V. Conclusions

In this paper, we proposed the linkage mechanism that reproduce horse-like flexible leg trajectories. The distance driver inserted to the linkage as function of muscle tendon unit and its constraint formulation introduced. The results presents detailed information of effect of changes of linear displacement in distance driver measured on velocity, acceleration and power consumption of driving link. The result shows that biologically inspired closed linkage mechanism driven by cyclic motion can be energy efficient and adaptable with the sudden change of the environment were presented by different modifiable leg trajectory. The validity of the horse leg mechanism was confirmed successfully in terms of both range of motion and kinematics. The important finding is that a kicking force is generated in the toe just before the grounding. This non-linear kinematic transmission may provide a hint to analyze adaptive capabilities in the animal locomotion even by the simple closed linkage without a complex actuator control system.

In addition, the motion analysis can be developed following two points. The first point is a consideration of replacement of elastic links in a part. According to the theory of the flexible multibody dynamics [27], our analysis seamlessly can be extended to the flexible multibody dynamics, which may improve the efficacy to absorb the ground reaction force when grounding of the leg. The second point is the ground reaction analysis to require an introduction of the extra component as the ground surface in the formulation of the multibody dynamics with multiple parameters such as tenderness and friction. The third point is the relationship between the torso and limbs. It is reflected to the condition with other legs at least, or including the ground reaction force. The torso height is depending on the motion pattern of four legs, which are called ambling gaits [28] and changes depending on the horse rider and its training. Therefore, the relationship between the torso and limbs is analyzed with a control theory of four legs, which can be discussed by the central pattern generator (CPG) [29].

References

[1] McGeer, T., "Passive Dynamic Walking," *The International Journal of Robotics Research*, vol. 9, no. 2, 1990, pp. 62–82.

[2] Campbell, D., Buehler, M., "Preliminary bounding experiments in a dynamic hexapod," In: *Experimental Robotics,* vol. VIII, 2003, pp. 612–621 Springer-Verlag.

[3] Gregorio, P., Ahmadi, M., Buehler, M., "Design, control, and energetics of an electrically actuated legged robot," *IEEE Trans. Syst. Man Cybern., Part B, Cybern.* vol. 27, 1997, pp. 626–634.

[4] Jin, B., Chen, C., Li, W., "Power consumption optimization for a hexapod walking robot," *J. Intell. Robot. Syst.* vol. 71, 2013, pp. 195–209.

[5] Jansen T., *The great pretender.* Rotterdam: 010 Publishers, 2007.

[6] K. Komoda, H. Wagatsuma, "Energy-efficacy comparisons and multibody dynamics analyses of legged robots with different closed-loop mechanisms," *Multibody Syst. Dyn.,* vol. 40, no. 2, 2017, pp. 123–153.

[7] Nikravesh, P.E., *Computer-Aided Analysis of Mechanical Systems,* Prentice Hall International, Englewood Cliffs, 1988.

[8] Haug, E.J.: *Computer Aided Kinematics and Dynamics of Mechanical Systems: Basic Methods,* vol. 1. Allyn and Bacon, Boston, 1989.

[9] Hildebrand, M., "Symmetrical Gaits of Horses," *Science,* Vol. 150, 1965, pp. 701-708.

[10] Hoyt, D. F., Taylor, C. R., "Gait and the energetic of locomotion in horses," *Nature*, vol. 292, no. 5820, 1981, pp. 239-240.

[11] Starke, S. D., Robilliard, J. J., Weller, R., Wilson, A. M., Pfau, T., "Walk–run classification of symmetrical gaits in the horse: a multidimensional approach," *J R Soc Interface.,* vol. 6, no. 33, 2009, pp. 335–342.

[12] Huang, T.-C., Huang, Y.-J., Lin, W.-C., "Real-time Horse Gait Synthesis," *Comp. Anim. Virtual Worlds 2013,* vol. 24, 2012, pp. 87–95.

[13] Fihl, P., Moeslund, T. B., "Invariant gait continuum based on the duty-factor," *Signal, Image and Video Processing*, vol. 3, 2009, pp. 391–402.

[14] Komoda, K., Wagatsuma, H., "Singular configurations analyses of the modifiable Theo Jansen-like mechanism by focusing on the Jacobian determinant—a finding limitations to exceed normal joint range of motion," In: *Proceedings of 2014 IEEE/ASME International Conference on Advanced Intelligent Mechatronics (AIM)*, 2014, pp. 76–81.

[15] Komoda, K., Wagatsuma, H., "A determinant analysis to detect the singularity of the extended Theo Jansen mechanism in the phase-rotation-amplitude parameter space," *J. Comput. Sci. Syst. Biol.* 9(1), 10–22 (2015)

[16] Nansai, Shunsuke, et al. "On a Jansen Leg with Multiple Gait Patterns for Reconfigurable Walking Platforms." *Advances in Mechanical Engineering*, Mar. (2015).

[17] Coros, S., Thomaszewski, B., Noris, G., Sueda, S., Forberg, M., Sumner, R. W., Matusik, W., Bickel, B., "Computational Design of Mechanical Characters," ACM Transactions on Graphics (TOG), 32(4): Article No. 83.

[18] Budras, K. D., Sack, W. O., Rock, S., Horowitz, A., Berg, R., Anatomy of the Horse, "Chapter 3: Pelvic Limb," In *Anatomy of the Horse*, pp. 23–39, London: Schluetersche, 2012

[19] Van Weeren, P.R., Van den Bogert, A.J., Hartman, A.B.W., Kersjes, A.W., "The role of the reciprocal apparatus in the hind limb of the horse investigated by a modified CODA-3 opto-electronic kinematic analysis system," *Equine Vet. J.* Suppl. 9, 95-100. (1990).

[20] Molenaar, B. J., "Kinematics of the Reciprocal Apparatus in the Horse," *Anatomia, Histologia, Embryologia*, vol. 12, 1983, pp. 278-287.

[21] Hildebrand, M, "The Mechanics of Horse Legs," *American Scientist,* vol. *75, no.* 6, 1987, pp. 594-601.

[22] Shabana, A.A. *Computational Dynamics, 3rd Edition*, United states: Wiley, 2009.

[23] Baumgarte, J., "Stabilization of constraints and integrals of motion in dynamical systems," *Comput. Methods Appl. Mech. Eng.* vol. 1, 1972, pp. 1–16.

[24] Ostermeyer, G.P., "On Baumgarte stabilization for differential algebraic equations," In: Haug, E.J., Deyo, R.C. (eds.) Real-Time Integration Methods for Mechanical System Simulations. *NATO ASI Series*, vol. F69, 1990, pp. 193–207. Springer, Berlin.

[25] Muller, M., "A novel classification of planar four-bar linkages and its application to the mechanical analysis of animal systems," *Philos. Trans. R. Soc. Lond.* B vol. 351, 1996, pp. 689-720.

[26] Shigley, J.E., "The mechanics of walking vehicles: a feasibility study: final report," *Technical reports*, The university of Michigan, UMRI Project 2859, 1960.

[27] Shabana, A.: Flexible Multibody Dynamics, "Review of Past and Recent Developments," *Multibody System Dynamics*, vol. 1, no. 2, 1997, pp. 189-222.

[28] Schmitt, D., Cartmill, M., Griffin, T. M., Hanna, J. B., Lemelin, P., "Adaptive value of ambling gaits in primates and other mammals," Journal of Experimental Biology, vol. 209, 2006, pp. 2042-2049.

[29] Guertin, P. A., "Central Pattern Generator for Locomotion: Anatomical, Physiological, and Pathophysiological Considerations," Front Neurol., vol. 3, 2013, Article 183.